Table 1 Comparison of static pressure obtained by pressure dots, PSP methods, and CFD

	Numbers of pressure dots					
	1	2	3	4	5	6
EUL	0.909	0.929	0.867	0.907	1.012	0.977
TRB	0.947	0.833	0.747	0.715	0.967	1.034
Taps	0.965	0.892	0.708	0.723	0.945	1.008
PSP	——	——	0.72	0.774	0.943	1.015

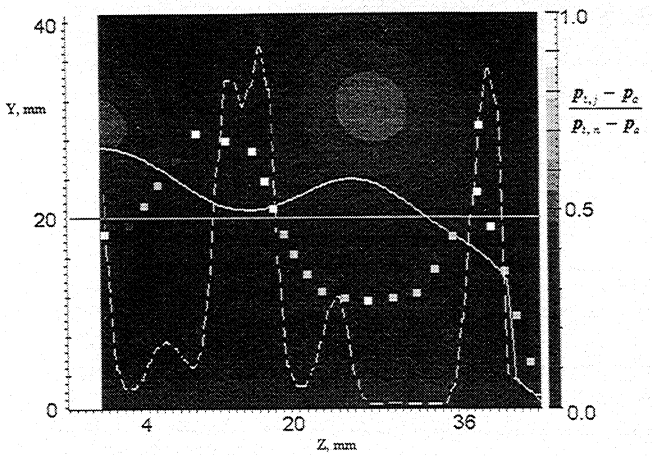

Fig. 4 Total pressure distribution at the exit section of ejector: ---, Euler; ——, turbulent viscosity; □, experiment.

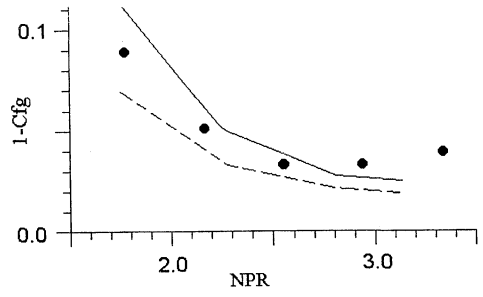

Fig. 5 Nozzle thrust losses: ---, Euler; ——, turbulent viscosity; ●, experiment.

onstrated, and the function of nondimensional total pressure $(p_{t,j} - p_a)/(p_{t,n} - p_a)$ is used. TRB data are compared with those of EUL and are depicted as having a black–white tone distribution. The chart in Fig. 4 shows the values of nondimensional total pressure along the white line in the middle of the figure. The solid line corresponds to the TRB data, the dashed line to the EUL ones, and the square markers are the experiment. It is obvious that the TRB data are in a poor qualitative agreement with the experiment. Turbulence viscosity in this case is too large to provide a good description of the mixture process after the lobes. This problem is the subject for future turbulence model investigations.

Comparison of the static pressure distribution along nozzle's side wall is shown in Table 1 for NPR = 2.75 (the averaged Mach number at the exit of the mixer is about 0.8). Experimental pressure distribution is obtained by the pressure taps with numbers 1–6[1] and by using pressure sensitive paints (PSP) technology. TRB data are much closer to the experiment (~5%) than those of EUL (up to 25%). Ejection caused by turbulent viscosity provides an additional rarefaction in the mixing area (dots 2 ÷ 4).

In Fig. 5, the TRB (solid line) and the EUL (dashed line) data for the thrust loss coefficient are compared with the experimental ones (●). When turbulence viscosity is taken into account, the computational curve is shifted and comes closer to experimental points. This indicates that ejection works. An extremely large shift shows that turbulence viscosity is too large and will result in additional thrust loss.

Conclusions

Results of calculations using a Favre-averaged Euler equation system closed by the $(q - \omega)$ model of turbulence show that 1) the main features of the flow in the nozzle mixer predicted earlier are confirmed, 2) the wake surface obtained in the TRB case is smoother than that in the EUL, 3) taking ejection into account improves the distribution of the static pressure on the wall, and 4) a detailed description of the total pressure distribution requires that the turbulent model be corrected.

Acknowledgments

This investigation was supported by the International Science and Technology Center in Moscow. Many thanks to S. Mikhailov who prepared the postprocessor's graphics and to M. Engulatova who worked with this article.

References

[1]Bosniakov, S., Fonov, S., Jitenev, V., Shenkin, A., Vlasenko, V., and Yatskevich, N., "Method for Noise Suppressing Nozzle Calculation and First Results of Its Implementation," *Journal of Propulsion and Power*, Vol. 14, No. 1, 1998, pp. 101–109.

[2]Coakley, T. J., "Turbulence Modeling Methods for the Compressible Navier-Stokes Equations," AIAA Paper 83-1693, July 1983.

[3]Dash, S., Weilersteen, G., and Vaglio-Laurin, R., "Compressibility Effects in Free Turbulent Shear Flows," Air Force Office of Scientific Research, TR-75-1436, 1975.

Development of a Strutjet Cold-Flow Mixing Experiment

David M. Spetman,* Clark W. Hawk,† and Marlow D. Moser‡
University of Alabama in Huntsville, Huntsville, Alabama 35899

Introduction

ROCKET-based combined cycle (RBCC) concepts attempt to improve the performance of launch vehicles at all points in the launch trajectory and make highly reusable launch vehicles a reality. The strutjet RBCC concept consists of a variable geometry duct with vertical struts inside that function in ducted rocket, ramjet, scramjet, and pure rocket modes.[1] These struts have rocket and turbine exhaust nozzles imbedded within them. The rocket flows induce an ejector effect with the ambient air at subsonic flight velocities. In ramjet and scramjet modes, the fuel-rich nozzle flows react with the ambient air, producing an afterburner effect. As shown in Fig. 1, the four primary rocket flows exit at the end of the strut with three turbine exhaust nozzles in between them. The strutjet is designed to mix the fuel-rich flows (rocket and turbine exhaust

Received Sept. 8, 1997; revision received June 27, 1998; accepted for publication July 6, 1998.

*Von Braun Propulsion Fellow, Propulsion Research Center, Department of Mechanical and Aerospace Engineering. Student Member AIAA.

†Director, Propulsion Research Center, also Professor, Department of Mechanical and Aerospace Engineering. Fellow AIAA.

‡Assistant Research Professor, Propulsion Research Center, Department of Mechanical and Aerospace Engineering. Member AIAA.

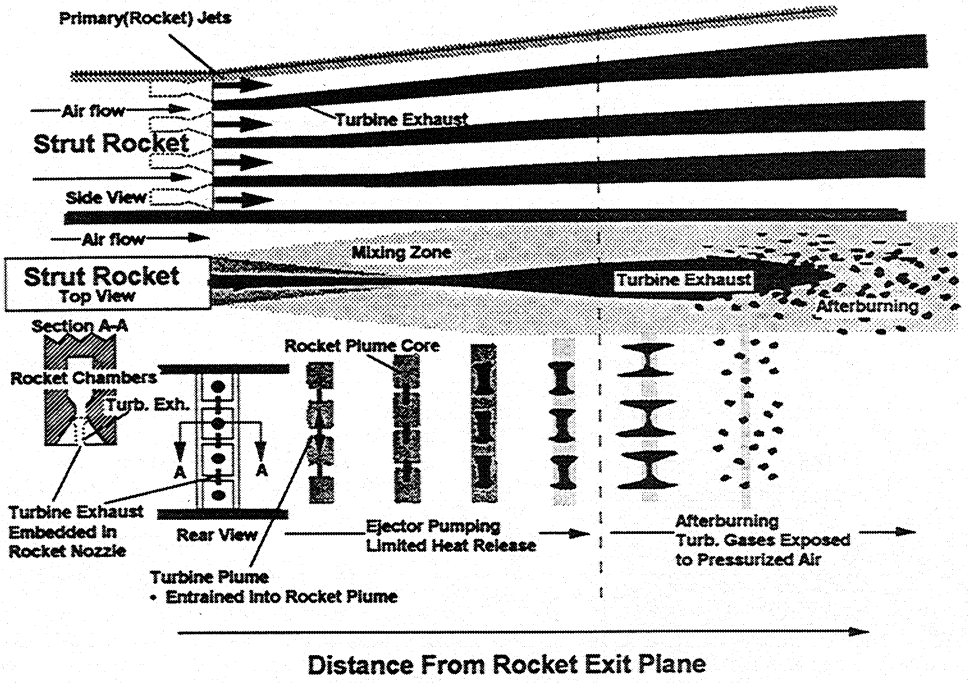

Fig. 1 Rocket and turbine exhaust mixing in the strutjet.[2]

gases) in the vertical direction before significant combustion occurs with the ambient air. After the hot, fuel-rich flows are mixed (and after the shear layers between the nozzle flows and the ambient air reach the walls of the duct), air-breathing combustion begins. The combustion products are expanded through the duct's nozzle that is provided by the engine and, to a large part, by the air frame.§ The objective of this paper is to present the development of an experiment that will determine the mixing characteristics of the strutjet rocket and turbine exhaust gases.

Approach

A scale model of the current strutjet design will be cold flow tested in a duct. The simulants will be heated and the nozzles will be designed to match the convective Mach number predicted for the full-scale strutjet nozzle flows to obtain similar mixing. The turbine nozzle gas will be seeded to trace the mixing of the turbine simulant with the rocket simulant.

Constraints

The main constraints on the design of the experiment were the similarity parameter, matching the geometric scale of a subscale test motor, (one-sixth of an engine for a vehicle that delivers a 25K lbm payload to the International Space Station) and the diagnostic technique. The parameter chosen to ensure mixing similarity between the model and full-scale prototype was the convective Mach number (M_c), developed by Papamoschou and Roshko[2] to correlate supersonic shear-layer growth rates. A derived variable, the convective velocity (U_c), is used to approximate the velocity of the large turbulent structures found in supersonic shear layers. As shown in Eq. (1), the convective velocity is calculated by weighting the velocities of two flows by the speeds of sound of the opposite flows and assumes 1) similar specific heat ratios [Eq. (1) is exact for $\gamma_1 = \gamma_2$], 2) equal total and static pressures at the shear layer, and 3) steady flow

$$U_C \approx \frac{a_2 U_1 + a_1 U_2}{a_1 + a_2} \tag{1}$$

§Bulman, M., private communication, Aerojet, Sept. 6, 1996.

$$M_{C_1} = \frac{U_1 - U_C}{a_1} \approx M_{C_2} = \frac{U_C - U_2}{a_2} \tag{2}$$

This approach makes the convective Mach number a compressibility-effect parameter and creates a coordinate system based on the motion of the large, dominant structures seen in turbulent flow. The convective Mach number can be calculated using either of the two flows as a reference flow [see Eq. (2)]; both methods are equal if both flows have the same specific heat ratio, are supersonic, and $M_c < 0.4$ (asymmetries become apparent above $M_c = 0.4$ because of compressibility effects).[3,4] In the full-scale, hot-flow strutjet, the convective Mach number between the rocket and turbine flows ($M_{c_{rt}}$) is approximately 0.6. The convective Mach number between the rocket and ambient airflows is 2.6, and the convective Mach number between the turbine and ambient airflows is 2.0. Because the experiment is a cold flow test, the convective Mach numbers associated with the exhaust gases and ambient air are impossible to achieve; however, $M_{c_{rt}} = 0.6$ is possible because it is a relative parameter between the hot rocket and turbine flows. Even then, the simulated rocket exhaust must be heated to achieve $M_{c_{rt}} = 0.6$. Because of this constraint, only the mixing between the rocket and turbine flows will be simulated with the experiment, and any contribution from ambient air mixing (and the ejector effect) will not be accurately simulated.

Optical Diagnostics

The overall goal of the diagnostics function is to provide both qualitative and quantitative information about the mixing behavior downstream of the strut rocket base. The quantitative results will provide a measure of the degree of mixing at various axial locations downstream of the strut rocket base, whereas the qualitative information obtained will provide valuable information about the structure of the flowfield. The design of the simulant supply systems and the geometry of the duct reflect the needs of the diagnostic technique that will be used on this project.

The potential methods investigated included Al_2O_3 seeding,[5] methanol/ethanol condensation,[6] and acetone fluorescence.[7] Al_2O_3 seeding was not chosen because of the increasing error from particle lag time the greater the distance from the nozzle

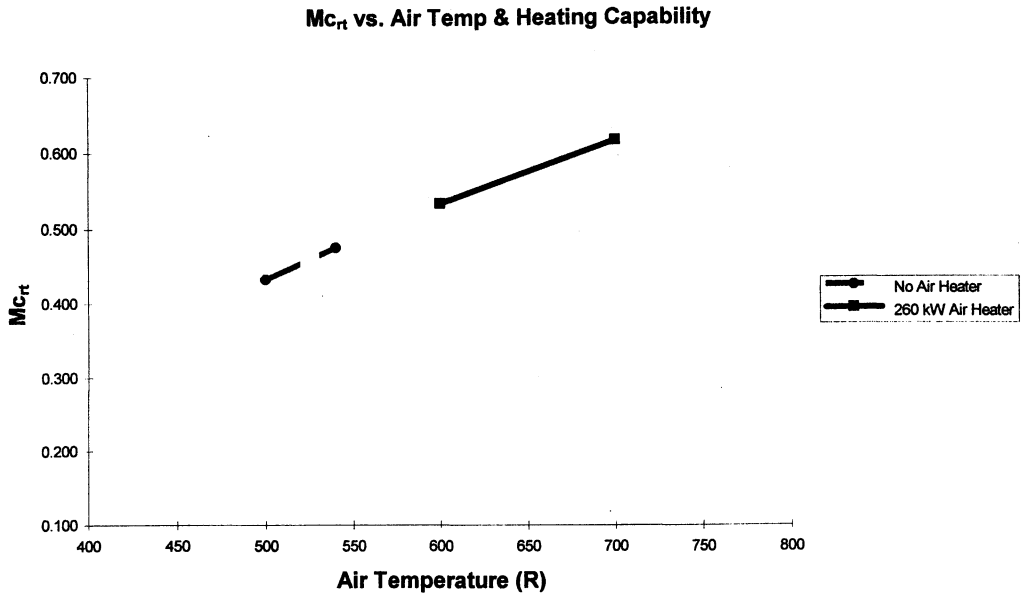

Fig. 2 Achievable convective Mach numbers.

exit. Methanol/ethanol was not chosen because of the possibility of droplet nucleation at the farthest sampling location. Acetone vapor fluorescence was chosen because of its strong signal properties and ease of seeding.

The acetone vapor is excited at a wavelength of 266 nm and the fluorescent signal is emitted over a wide spectral range (~350 to 550 nm). The fluorescent signal will be collected over a bandwidth of 485–495 nm, eliminating interference from scattered laser light. Acetone fluorescence is linear with respect to incident laser intensity and acetone mole fraction.[7] Collision quenching of acetone fluorescence is intramolecular.[7] The fluorescence is, therefore, independent of temperature and local gas composition. Thus, quantitative information is readily obtained from the collected images.

The acetone fluorescence has a lifetime of less than 4 ns. Acetone also phosphoresces at wavelengths similar to the fluorescence, albeit at a much greater lifetime of about 200 μs. The phosphorescence interference is rendered negligible by the gating of the intensified camera at 10 μs. This also eliminates background interference.

The Nd:YAG laser output of 1064 nm is frequency quadrupled to produce a 266-nm laser beam. The 1064- and 532-nm components of the beam will be separated into a beam dump while the 266-nm beam is sent to the test section. The beam is formed into a laser sheet approximately 2 in. high and 500 μm thick by a series of cylindrical lenses. The beam then passes through a 4 in. × 4 in. fused silica window into the duct. The beam traverses the model cross section of concern and passes through the 4 in. × 4 in. window on the other side.

Working Fluids Selection

An iterative design process was used to determine which gases should be used as simulants for the nozzle flows. A spreadsheet, using quasi-one-dimensional nozzle flow equations,[8] was used to calculate the $M_{c_{rt}}$ for a variety of gases and nozzle conditions. The turbine simulant has to be heated to make sure the acetone would remain vaporized in the turbine flow. This greatly affected the ability of the gases to achieve $M_{c_{rt}} = 0.6$, and stressed the power requirement of the rocket simulant heater.

The first gases explored were air and nitrogen, as rocket and turbine simulants, respectively. The air/nitrogen combination could not reach $M_{rt} = 0.6$, even when the exit temperature of the turbine nozzle was below the condensation point of acetone. Helium was also considered for the turbine simulant, but the combination could not achieve $M_{c_{rt}} = 0.6$ because of helium's higher γ and lower molecular weight. A combination using helium as a rocket simulant and air or nitrogen as a turbine simulant could reach $M_{c_{rt}} = 0.6$; however, helium is an expensive gas that requires special piping and sealing considerations to prevent leaks. Carbon dioxide was examined as a simulant for the turbine nozzle. Carbon dioxide has a lower γ and a higher molecular weight than air (the rocket simulant), which made it a better turbine simulant than nitrogen.

An air compressor will pump a 500-ft^3 tank to 1100 psi. This tank will be blown down to 925 psi, supplying the model with high-pressure air as the rocket simulant. Figure 2 shows the achievable $M_{c_{rt}}$ of this air-supply tank with and without the use of a 260-kW heater. Because the carbon dioxide exiting the turbine nozzle must remain above the condensation temperature of acetone, the air will be heated to over 600°R with the 260-kW heater to reach a $M_{c_{rt}}$ close to 0.6.

Model Design

The baseline model design was chosen at one-sixth geometric scale to facilitate comparison of cold flow data with subscale motor firings. A configuration with two rocket nozzles and one turbine nozzle was elected to minimize the mass flow rate requirements. The simulants will be air (rocket) and carbon dioxide (turbine). The rocket nozzle will have a chamber temperature of at least 600°R, a chamber pressure of 600 psi, a mass flow rate of 4.0 lbm/s, and an area ratio of 4.5. The rocket nozzles are designed to exit at atmospheric pressure (14.7 psi). The turbine nozzle will have a chamber temperature of 760°R, a chamber pressure of 90 psi, a mass flow rate of 0.09 lbm/s, and an area ratio of 1.126. The turbine nozzle was designed to have an exit pressure greater than the rocket nozzle wall pressure at their point of intersection to facilitate the vertical expansion and mixing of the turbine exhaust gas into the rocket exhaust gas. The exit temperature of the turbine exhaust must be greater than 590°R to avoid condensation of acetone in the flow within the viewing area.

Figure 3 shows the side and rear views of the stainless-steel model. The strut is only 1 in. wide and 6.5 in. tall. The model will be tested in a duct with internal dimensions of 4 in. high and 3.4 in. wide. The small duct width will create measurable air entrainment. The primary rocket nozzles have circular chambers and throats that transition to ~0.83 × 0.83-in.^{2} exits as in the full-scale version. The turbine nozzle is a rectangular duct that is 0.49 × 0.09 in. at the exit. The turbine exhaust nozzle intersects the wall of the rocket nozzles about 0.23 in. before the rocket nozzle exit plane. These nozzles have the

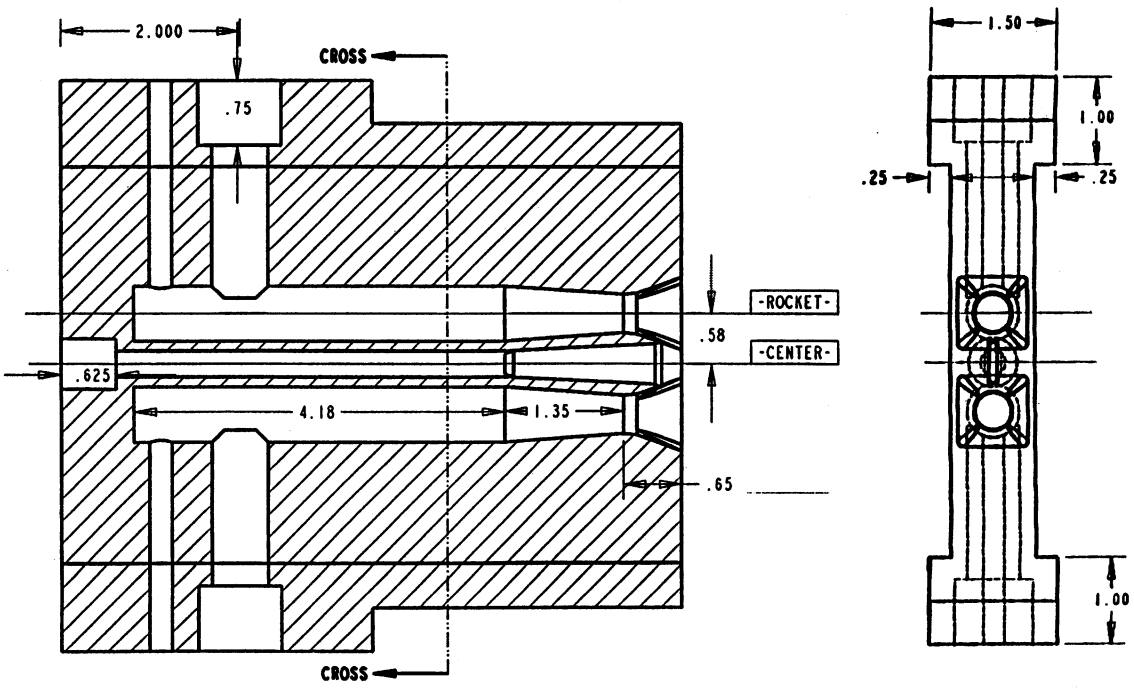

Fig. 3 Side and rear views of the cold-flow test model.

same divergence angles currently envisioned for full-scale models. Three additional models will offer variations from this baseline design.

The effect of the ingested flow upon the turbine/rocket flow mixing is not understood at this time. The lateral rate of spreading of the turbine exhaust stream as a function of distance downstream is expected to provide a measure of this effect.

Test Plan

The first item in the test program will be verification of the diagnostic method. Acetone will be seeded in the turbine simulant at increasing levels to determine when and if it will condense. The laser and camera will be positioned and tested. Pressure measurements will be carefully taken to determine if the system reaches a steady state, and pitot probes will sample the nozzle exhaust to verify predicted nozzle exit conditions. Pitot probes will also be used to sample the ingested airflow to understand its behavior and possible impact on mixing. Temperature measurements will also be made in the chamber to estimate delivered $M_{c_{rt}}$. Once the checkout is complete, the primary testing will begin. The rocket chamber temperature will be varied between 600 and 700°R with the 260-kW air heater. This will change the convective Mach number from around 0.5 to slightly more than 0.6. Acetone-based planar laser-induced fluorescence (PLIF) images will be taken for a least three convective Mach numbers to see how the mixing varies with $M_{c_{rt}}$. Data will be taken at the rocket nozzle exit plane, and at L/D (distance from the exit plane/nozzle exit diameter) of 9 and 18. It is expected that complete mixing will be achieved by an L/D of 18. The stations selected provide an opportunity to observe the mixing process of the turbine and rocket exhaust plumes from the exit plane to where complete mixing is envisioned. At least two tests at each measurement location and $M_{c_{rt}}$ will be taken to enable statistical analysis. There is a maximum of four models planned for testing, including the baseline model.

Conclusions

This experiment meets the established requirements: a convective Mach number at 0.6 is achievable and the model's scale is not smaller than one-sixth. The experiment uses heated air as the rocket exhaust simulant and heated carbon dioxide as the turbine simulant. Acetone-based PLIF will be used to visualize and quantitatively evaluate the rocket and turbine exhaust flows. The test results will be used to complement hot-fire testing.

Acknowledgments

NASA Marshall Space Flight Center provided funding and technical support for this mixing experiment under Cooperative Agreement NCC8-123. Aerojet assisted with the planning of the experiment, and Rapid Tech Engineering is constructing the test model.

References

[1]Bulman, M., and Siebenhaar, A., "The Strutjet Engine: Exploding the Myths Surrounding High Speed Airbreathing Propulsion," AIAA Paper 95-2475, July 1995.

[2]Papamoschou, D., and Roshko, A., "The Compressible Turbulent Shear Layer: An Experimental Study," *Journal of Fluid Mechanics*, Vol. 197, 1988, pp. 453–477.

[3]Papamoschou, D., "Structure of the Compressible Turbulent Shear Layer," *AIAA Journal*, Vol. 29, 1991, pp. 680, 681.

[4]Bunyajitradulya, A., and Papamoschou, D., "Acetone PLIF Imaging of Turbulent Shear Layer Structure at High Convective Mach Number," AIAA Paper 94-0617, 1994.

[5]Eaton, A. R., et al., "Development of a Full-Field Planar Mie Scattering Technique for Evaluating Swirling Mixers," *Experiments in Fluids*, Vol. 21, 1996, pp. 325–330.

[6]Clemens, N. T., and Mungal, M. G., "A Planar Mie Scattering Technique for Visualizing Supersonic Mixing Flows," *Experiments in Fluids*, Vol. 11, 1991, pp. 175–185.

[7]Lozano, A., Yip, B., and Hanson, R. K., "Acetone: A Tracer for Concentration Measurements in Gaseous Flows by Planar Laser-Induced Fluorescence," *Experiments in Fluids*, Vol. 13, 1992, pp. 369–376.

[8]Sutton, G., *Rocket Propulsion Elements*, 6th ed., Wiley, New York, 1992.